



Aligned MHD of Ferrofluids with Convective Boundary Condition past an Inclined Plate

Mohd Rijal Ilias^{1,2*}, Noraihan Afiqah Rawi², Nur Sa'aidah Ismail¹, Sharidan Shafie²

¹Faculty of Computer and Mathematical Sciences, Universiti Teknologi MARA, Malaysia

²Department of Mathematical Sciences, Faculty of Science, Universiti Teknologi Malaysia, Johor Bahru, Johor, Malaysia

*Corresponding author E-mail: rijal_rs@hotmail.com

Abstract

The numerical investigation is carried out for the MHD free convection laminar boundary layer flow that allows heat transfer of an electrically conducting Fe₃O₄-kerosene and Fe₃O₄-water-based ferrofluids. For this, an inclined plate is employed that has aligned effect as well as transverse magnetic field effect. Suitable similarity transformations are used to convert governing partial differential equations into a coupled nonlinear ordinary differential equation. The Keller Box method, a well-known explicit finite difference scheme is then employed to solve transformed equations numerically. For different values of physical parameters, a detailed parametric study is conducted. Means of graphs are extrapolated to determine the effects of all these parameters over temperature and the flow field. For various values of physical parameters, the numerical values are obtained and tabulated for skin friction coefficient and the rate of heat transfer as well. Comparisons with previously published work are performed and excellent agreement is obtained.

Keywords: Aligned MHD; Convective boundary condition; Ferrofluids; Free convection; Inclined plate.

1. Introduction

Nanofluids have wide application in various fields and have provided significant importance towards enhancement of heat transfer. Their applications include desalination, cavity problem, solar thermal collector and so on [1-2]. Ferrofluids are magnetic nanofluids, which consist of a colloidal mixture of magnetic nanoparticles with size in the range of 10–20 nm and base liquid. Ferrofluids' magnetic features are comparable to those of bulk magnetic materials and the yellow retaining common Newtonian fluids' flow characteristic. As indicated by several studies, outstanding heat transfer enhancement can be achieved by employing nanofluids as coolants when compared with ordinary fluids [3-4]. Magneto-hydrodynamic (MHD) deals with the study of electrically conducting fluids that can move around in a magnetic field. An electric current is induced in the fluid when there is a change in the magnetic field that cuts the moving fluid. Studies have been reviewed for laminar flow over an inclined plate. It should be noted that in this line, various investigations are conducted. An incompressible nanofluid's steady mixed convection boundary layer flow was investigated by [5] along an inclined plate that was embedded in a porous medium. In their study, it was observed that Nusselt number decreased with rise in thermophoresis number or Brownian motion number whereas increasing the plate's angle led to increase in Nusselt number. Also, the free convection flow from an isothermal plate that was inclined horizontally at a small angle was studied by [6]. Recently, the numerical solution of MHD mixed convection nanofluid flow was analysed by [7] over an inclined stretching plate. They considered the heat generation and suction effects. Numerous authors [8-9] have investigated the issues associated with the MHD boundary layer by considering different effects.

Many industrial applications, natural processes and chemical processing systems are faced with the free convection processes that involve combination mechanism of mass and heat transfer. In [10] who started the convection flow study, used an integral method to make a technical note on transient free convection flow's similarity solution past a semi-infinite vertical plate. In [11] studied the unsteady free convection flow on an isothermal surface near the attachment's three-dimensional stagnation point. However, to the extent of authors' knowledge, attempts are yet to be made to address the issues of aligned MHD free convection heat transfer flow regarding ferrofluids over an inclined plate with convective boundary condition. Hence, a study was conducted in an attempt to understand free convection boundary layer flow over an inclined plate for two ferrofluids, namely Fe₃O₄-kerosene and Fe₃O₄-water.

2. Mathematical Formulation

Consider the steady two-dimensional, incompressible, laminar, hydromagnetic free convection of ferrofluids flow over an inclined plate with aligned and transverse magnetic field. The plate is inclined at an angle of inclination γ measured in the clockwise direction and situated in an otherwise quiescent ambient fluid at temperature T_∞ . The gravitational acceleration g is acting downward.

The physical coordinates (x, y) are chosen such that x -axis is chosen along the plate and the y -axis is measured normal to the surface of the plate (Figure 1). Water and kerosene are used as the base fluids with magnetite (Fe₃O₄) as a nanoparticles. The base fluids and nanoparticles are in thermal equilibrium and no slip

occurs between them. The spherical shaped nanoparticles are considered. The viscous dissipation and radiation are neglected in the analysis.

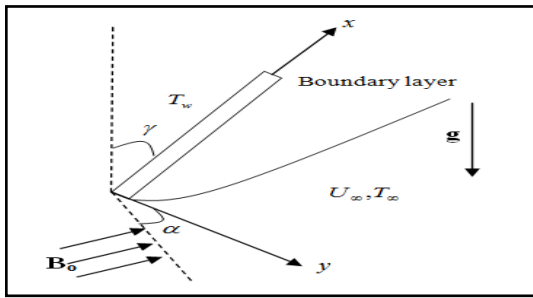


Fig. 1: Geometry of the problem

Under the above assumptions and following [12], the equations of MHD boundary layer flow are

$$\frac{\partial u}{\partial x} + \frac{\partial v}{\partial y} = 0 \tag{1}$$

$$u \frac{\partial u}{\partial x} + v \frac{\partial u}{\partial y} = \frac{\mu_{nf}}{\rho_{nf}} \frac{\partial^2 u}{\partial y^2} + \frac{(\rho\beta)_{nf}}{\rho_{nf}} g \cos \gamma (T - T_\infty) - \frac{\sigma B^2(x)}{\rho_{nf}} \sin^2 \alpha (u - U_\infty) \tag{2}$$

$$u \frac{\partial T}{\partial x} + v \frac{\partial T}{\partial y} = \alpha_{nf} \frac{\partial^2 T}{\partial y^2} \tag{3}$$

The boundary conditions for the velocity and temperature of this problem are given by

$$u(x,0) = 0, \quad v(x,0) = 0, \quad -k_f \frac{\partial T(x,0)}{\partial y} = h_f (T_f - T(x,0)), \tag{4}$$

$$u(x,\infty) = U_\infty, \quad T(x,\infty) = T_\infty.$$

where u and v are the x (along the plate) and the y (normal to the plate) component of velocities respectively T is the temperature of the ferrofluids, T_w is the ambient temperature of the ferrofluids, U_∞ is the constant free stream velocity and σ is the electrical conductivity. The transverse magnetic field assumed to be a function of the distance from the origin is defined as $B(x) = B_0 x^{-\frac{1}{2}}$ with $B_0 \neq 0$, where x is the coordinate along the plate and B_0 is the magnetic field strength. The effective properties of ferrofluids may be expressed in terms of the properties of base fluids, nanoparticles and the volume fraction of solid nanoparticles as follow [13, 18]

$$\begin{aligned} \rho_{nf} &= (1-\phi)\rho_f + \phi\rho_s, & \mu_{nf} &= \frac{\mu_f}{(1-\phi)^{2.5}}, \\ (\rho C_p)_{nf} &= (1-\phi)(\rho C_p)_f + \phi(\rho C_p)_s, & (\rho\beta)_{nf} &= (1-\phi)(\rho\beta)_f + \phi(\rho\beta)_s, \\ \alpha_{nf} &= \frac{k_{nf}}{(\rho C_p)_{nf}}, & \frac{k_{nf}}{k_f} &= \frac{k_s + 2k_f - 2\phi(k_f - k_s)}{k_s + 2k_f + \phi(k_f - k_s)}. \end{aligned} \tag{5}$$

where ρ_{nf} is the effective density, ϕ is the solid volume fraction, ρ_f and ρ_s are the densities of pure fluid and nanoparticles respectively μ_f is the dynamic viscosity of the base fluids, μ_{nf} is the effective dynamic viscosity, $(\rho C_p)_{nf}$ is the heat capacity of the ferrofluids, $(\rho C_p)_f$ is specific heat parameters of the base fluids, $(\rho C_p)_s$ is the specific heat parameters of nanoparticles, $(\rho\beta)_{nf}$ is

the thermal expansion coefficient, α_{nf} is the thermal diffusivity of the ferrofluids, k_{nf} is the thermal conductivity of the ferrofluids, $(\rho C_p)_{nf}$ is the heat capacity of the ferrofluids, k_f and k_s are thermal conductivities of the ferrofluids and nanoparticles. The continuity in (1) is satisfied by introducing a stream function $\psi(x, y)$ below

$$u = \frac{\partial \psi}{\partial y}, \quad v = -\frac{\partial \psi}{\partial x}. \tag{6}$$

The following similarity variables are introduced

$$\eta = y \sqrt{\frac{U_\infty}{\nu_f x}} = \frac{y}{x} \sqrt{\text{Re}_x}, \quad \psi = \nu_f \sqrt{\text{Re}_x} f(\eta), \quad \theta = \frac{T - T_\infty}{T_w - T_\infty}. \tag{7}$$

where η is the similarity variable, $\text{Re}_x = U_\infty x / \nu_f$ is the Reynolds number, $f(\eta)$ the non-dimensional stream function and $\theta(\eta)$ the non-dimensional temperature.

On the use in (5), (6) and (7), (2) and (3) reduce to the following nonlinear system of ordinary differential equations:

$$\begin{aligned} f''' + (1-\phi)^{2.5} \left(1 - \phi + \phi \left(\frac{\rho_s}{\rho_f} \right) \right) \frac{1}{2} f f'' + (1-\phi)^{2.5} M (1-f') \sin^2 \alpha \\ + (1-\phi)^{2.5} \left(1 - \phi + \phi \left(\frac{(\rho\beta)_s}{(\rho\beta)_f} \right) \right) Gr_x \theta \cos \gamma = 0 \end{aligned} \tag{8}$$

$$\left(\frac{k_{nf}}{k_f} \right) \theta'' + \text{Pr} \left(1 - \phi + \phi \left(\frac{(\rho C_p)_s}{(\rho C_p)_f} \right) \right) f \theta' = 0 \tag{9}$$

subjected to the boundary conditions in (4) which become

$$\begin{aligned} f(0) = 0, \quad f'(0) = 0, \quad \theta'(0) = -Bi_x (1 - \theta(0)), \\ f'(\eta) = 1, \quad \theta(\eta) = 0, \quad \text{as } \eta \rightarrow \infty. \end{aligned} \tag{10}$$

where primes denote differentiation with respect to η , $M = \sigma B_0^2 / \rho U_\infty$ is the magnetic parameter, $Gr_x = g \beta_f (T_w - T_\infty) x / U_\infty^2$ is the local Grashof number and $\text{Pr} = (\mu C_p)_f / k_f$ is the Prantl number. In order to have a true similarity solution, the parameter Gr_x must be constant and independent of x . This condition will be satisfied if the thermal expansion coefficient β_f proportional to x^{-1} . Hence, assume [14] $\beta_f = a x^{-1}$ where a is a constant but have the appropriate dimension. Substituting $\beta_f = a x^{-1}$ into the parameter Gr_x will result

$$Gr = \frac{ag(T_w - T_\infty)}{U_\infty^2}.$$

The quantities of engineering interest are the skin-friction coefficient, C_f at the surface of the plate and local Nusselt number, Nu_x which are defined as:

$$C_f = \frac{\tau_w}{\rho_f U_\infty^2}, \quad Nu_x = \frac{xq_w}{k_f (T_w - T_\infty)}, \tag{11}$$

where τ_w is the wall skin friction or shear stress at the plate and q_w is the heat flux from the plate which given by:

$$\tau_w = \mu_{nf} \left(\frac{\partial u}{\partial y} \right)_{y=0}, \quad q_w = -k_{nf} \left(\frac{\partial T}{\partial y} \right)_{y=0} \quad (12)$$

Substituting in (10) into (15) and using (14)

$$\frac{C_f}{(Re_x)^{\frac{1}{2}}} = \frac{1}{(1-\phi)^{2.5}} f'(0), \quad \frac{Nu_x}{(Re_x)^{\frac{1}{2}}} = -\frac{k_{nf}}{k_f} \theta'(0) \quad (13)$$

3. Results and Discussion

To solve the normalised boundary layer equations, an efficient Keller Box method is employed and an elaborate discussion is provided for the effects of material parameters on the heat transfer characteristics and flow field. To the system's pertinent parameters, physically realistic numerical values were assigned to gain meaningful insights from the flow structure relating to temperature, velocity, reduced Nusselt number and skin friction coefficient. For this, two different base fluids are considered namely kerosene and water with magnetic nanoparticles, Fe_3O_4 . Table 1 is referred to know the thermophysical properties of kerosene, water and Fe_3O_4 .

Table 1: Thermophysical properties of base fluids and nanoparticles [3, 15]

Physical Properties	Water	Kerosene	Fe_3O_4
$\rho (kg/m^3)$	997.1	780	5200
$C_p (J/kgK)$	4179	2090	670
$k (W/mK)$	0.613	0.149	6
$\beta \times 10^{-5} (K^{-1})$	21	99	1.3

To validate the numerical method's accuracy, a direct comparison was made with the previously reported numerical results of [3, 16] for Fe_3O_4 -kerosene and Fe_3O_4 -water and aligned magnetic field parameter and in the absence of free convection parameter. Based on Table 2, the present results are observed to be in good agreement with those of the earlier findings.

Table 2: Comparison of the skin friction coefficient

	Volume Fraction	Skin Friction ($Gr_x = 0, \alpha = 90^\circ, \gamma = 0^\circ, M = 0$)		
		[19]	[3]	Present
Pure Water	0	0.3321	0.33206	0.332059
Fe_3O_4 -water	0.01	-	0.34324	0.343271
	0.2	-	0.59517	0.595192
Pure Kerosene	0	-	-	0.332059
Fe_3O_4 -kerosene	0.01	-	0.34557	0.345611
	0.2	-	0.63950	0.640265

As illustrated in Figure 2, the influence of magnetic field's inclined angle on temperature and velocity profiles of both Fe_3O_4 -kerosene and Fe_3O_4 -water ferrofluids are observed. It is concluded that enhanced velocity profiles and reduced temperature profiles in the aligned angle are achieved for both ferrofluids. Further, a decline in the momentum boundary layer and the thermal boundary layer is seen with increasing α in the case of both ferrofluids. This could be due to the strengthening of the applied magnetic field causing an increase in the value of aligned angle ($0^\circ \leq \alpha \leq 90^\circ$) in the plate. At $\alpha = 90^\circ$, this aligned magnetic field behaves like a transverse magnetic field and the magnetic field

attracts nanoparticles as a result of change in the aligned magnetic field's positions.

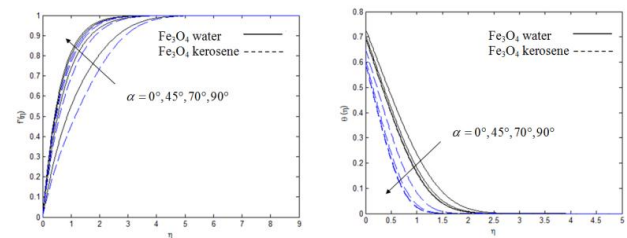


Fig. 2: Effect of aligned magnetic field parameters on the (a) velocity and (b) temperature profiles.

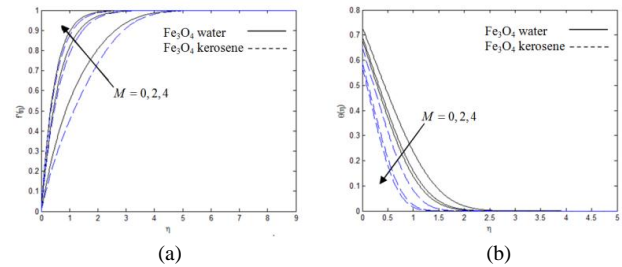


Fig. 3: Effect of magnetic strength parameters on the (a) velocity and (b) temperature profiles.

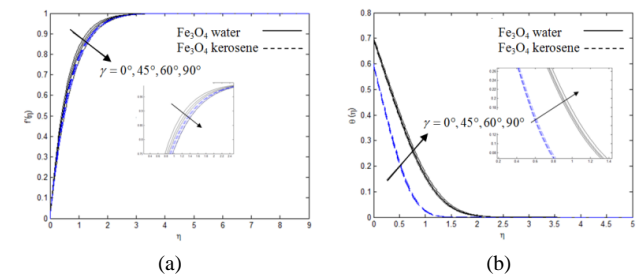


Fig. 4: Effect of inclined plate parameters on the (a) velocity and (b) temperature profiles.

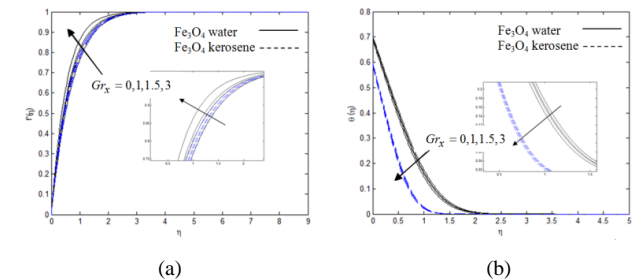


Fig. 5: Effect of local Grashof number on the (a) velocity and (b) temperature profiles.

As observed in Figure 3, increase in magnetic field parameter causes monotonic rise in the fluid velocity profiles along with a decrease in temperature. Moreover, for both ferrofluids, a decrease in thermal boundary layer and momentum can be seen for both ferrofluids.

Figure 4 shows a deceleration occurring in the velocity of ferrofluids with increase in the inclination of plate γ . The plate assumes a vertical position if $\gamma = 0^\circ$ while it is horizontal if $\gamma = 90^\circ$. For $\gamma = 90^\circ$, the gravitational effect is minimum while it is maximum for $\gamma = 0^\circ$. This behavior in the flow velocity is accompanied by strong increases in the fluid temperature. An increase of γ causes increase in the momentum and thermal boundary layer.

For computations, positive values of local Grashof number $Gr_x > 0$ are employed which corresponds to the cooling issue with regards to the application. Most engineering applications often encounter the cooling issue. From Figure 5, the thicknesses of thermal and

momentum boundary layers decrease with rise in Gr_x due of the buoyancy effect.

Figure 6 presents a graphical representation with respect to the velocity for different volume fraction values. For both ferrofluids (Fe_3O_4 -kerosene and Fe_3O_4 -water), the velocity in the boundary layer decreases with increase in volume fraction. This is caused by the increase in the number of collisions amongst solid particles, which consequently result in the velocity reduction of ferrofluids. For temperature distribution, temperature as well as the thermal boundary layer thickness are enhanced with increase in solid volume fraction values of nanoparticles. As the distance increases from the boundary, the distribution asymptotically moves towards zero. This is in agreement with the physical behaviour that states increase in thermal conductivity as well as thickness of the thermal boundary layer with increase in the volume fraction of Fe_3O_4 -kerosene and Fe_3O_4 -water.

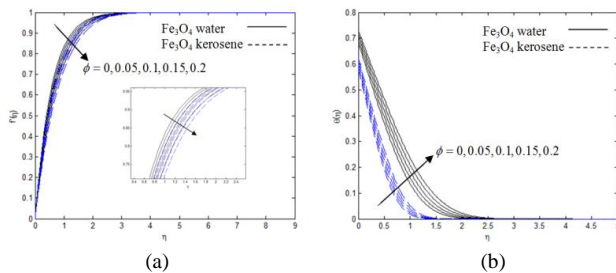


Fig. 6: Effect of volume fraction of nanoparticles on the (a) velocity and (b) temperature profiles.

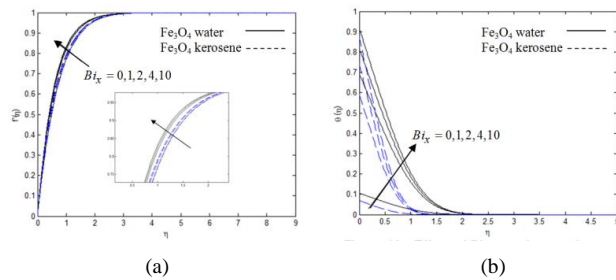


Fig. 7: Effect of Biot number on the (a) velocity and (b) temperature profiles.

Figure 7 shows the effect of Biot number on velocity and temperature field. Velocity increase when Bi_x increases while momentum boundary layer decreases. It is also found that both the plate surface and the nanofluids temperature increase when Bi_x is increased. This leads to an increase in thermal boundary layer thickness. As the value of parameter Bi_x increases, the intensity of convective heating on the plate surface increases which leads to an increasing rate of convective heat transfer from the hot fluid on the lower surface of the plate to the ferrofluids on the upper surface. The graph also reveals that temperature increases rapidly near the surface due to the increasing values of Bi_x . Thermal boundary layer for Fe_3O_4 -water is higher compare to Fe_3O_4 -kerosene.

From Table 3, one can notice that the skin friction coefficient at the wall increase in magnitude with an increase in $\alpha, M, \gamma, \phi, Gr_x, Bi_x$ of nanoparticles for both ferrofluids. It is noticed that, the highest wall shear stress occurs when magnetic strength increase. It is observed from Table 4, similar pattern occurs for Nusselt number and the highest rate of heat transfer occurs when volume fraction of nanoparticles increase. Heat transfer rate in Fe_3O_4 - kerosene is more compare to Fe_3O_4 - water based on Nusselt Number.

4. Conclusion

The problem of MHD free convection boundary layer flow of a ferrofluids through an inclined plate subjected to magnetic field has been analyzed. The following results were investigated

- (i) The velocity profiles of both ferrofluids increase with an increase in α, M, Gr_x, Bi_x . An increase in angle of γ and ϕ of nanoparticles results in decline of the velocity profiles for both ferrofluids.
- (ii) An increase in γ, ϕ, Bi_x of nanoparticles enhances the temperature profiles of both ferrofluids. The temperature profiles of both ferrofluids decrease with an increase in α, M, Gr_x .
- (iii) Increasing of all parameters except for angle of inclined plate increase the skin friction and heat transfer rate of both ferrofluids.
- (iv) In general, heat transfer rate in Fe_3O_4 - kerosene ferrofluid is more compare with Fe_3O_4 - water ferrofluid.

Table 3: Variation in skin friction coefficient and Nusselt number for Fe_3O_4 -water ferrofluids.

α	M	γ	ϕ	Gr_x	Bi_x	$C_f (Re_x)^{\frac{1}{2}}$	$Nu_x (Re_x)^{\frac{1}{2}}$
0°	2	45°	0.05	1.5	2	0.919410	0.597104
45°						1.456871	0.654261
90°						1.823751	0.679963
90°	0					0.919410	0.597104
90°	2					1.823751	0.679963
90°	4					2.382136	0.708723
90°		0°				1.933399	0.686825
90°		45°				1.823751	0.679963
90°		60°				1.744614	0.674854
90°			0			1.708704	0.634514
90°			0.05			1.823751	0.679963
90°			0.20			2.260842	0.818886
90°				0		1.547370	0.661491
90°				1.5		1.823751	0.679963
90°				3		2.084362	0.695890
90°					0.1	1.590073	0.099837
90°					4	1.871876	0.806364
90°					10	1.910155	0.908556

Table 4: Variation in skin friction coefficient and Nusselt number for Fe_3O_4 -kerosene ferrofluids.

α	M	γ	ϕ	Gr_x	Bi_x	$C_f (Re_x)^{\frac{1}{2}}$	$Nu_x (Re_x)^{\frac{1}{2}}$
0°	2	45°	0.05	1.5	2	0.738405	0.795059
45°						1.337266	0.893361
90°						1.725440	0.932941
90°	0					0.738405	0.795059
90°	2					1.725440	0.932941
90°	4					2.304673	0.975976
90°		0°				1.795721	0.938137
90°		45°				1.725440	0.932941
90°		90°				1.549813	0.919347
90°			0			1.616130	0.836034
90°			0.15			1.986612	1.143616
90°			0.20			2.14440	1.258602
90°				0		1.549813	0.919347
90°				1.5		1.725440	0.932941
90°				3		1.892935	0.945114
90°					0.1	1.570624	0.106673
90°					4	1.769136	1.176416
90°					10	1.808015	1.396788

Acknowledgement

This work is financially supported by the Fundamental Research Grant Scheme (FRGS) vot number 1533 under the Ministry of Higher Education Malaysia.

References

- [1] JM Wu & J Zhao. A review of nanofluid heat transfer and critical heat flux enhancement – Research gap to engineering application, *Progress in Nuclear Energy*, 66, (2013), 734–743.
- [2] AM Hussein, KV Sharma, RA Bakar & K Kadirgama. A review of forced convection heat transfer enhancement and hydrodynamic characteristics of a nanofluid, *Renewable and Sustainable Energy Reviews*, 29, (2014), 734–743.
- [3] WA Khan, ZH Khan & RU Haq. Flow and heat transfer of ferrofluids over a flat plate with uniform heat flux, *European Physical Journal Plus*, 130, 86, (2015).
- [4] J Philip et al. Enhancement of thermal conductivity in magnetite-based nanofluid due to chainlike structures, *Applied Physics Letters*, 91, (2007), 203108.
- [5] P Rana, R Bhargava & OA Beg. Numerical Solution for Mixed Convection Boundary Layer Flow of a Nanofluid along an Inclined Plate Embedded in a Porous Medium, *Computers and Mathematics with Applications*, 64, (2012), 2816–2832.
- [6] MA Hossain, I Pop & M Ahmad. MHD free convection flow from an isothermal plate, *Journal Theoretical and Applied Mechanics*, 1, (1996), 194–207.
- [7] SP Anjali Devi & P Suriyakumar. Numerical Investigation of Mixed Convective Hydromagnetic Nonlinear Nanofluid Flow Past an Inclined Plate, *AIP Conference Proceedings*, 1557, (2013), 281–285.
- [8] R Srinivas, K Naikoti & Mohammad Mehdi Rashidi. MHD flow and heat transfer characteristics of Williamson nanofluid over a stretching sheet with variable thickness and variable thermal conductivity, *Transactions of A. Razmadze Mathematical Institute* (2017).
- [9] K Vajravelu, KV Prasad, CO Ng & Hanumesh Vaidya. MHD squeeze flow and heat transfer of a nanofluid between parallel disks with variable fluid properties and transpiration, *International Journal of Mechanical and Materials Engineering*, 12, 1, (2017), 9.
- [10] S Ostrach. An Analysis of laminar free convection flow and heat transfer about a flat plate parallel to the direction of the generating body force, Technical Note, NACA Report, Washington (1952).
- [11] DB Ingham, JH Merkin & I Pop. Unsteady free convection of a stagnation point of attachment on an isothermal surface, *International Journal of Mathematics and Mathematical Sciences*, 7, 3, (1984), 599–614.
- [12] RK Tiwari & MK Das. Heat transfer augmentation in a two-sided lid-driven differentially heated square cavity utilizing nanofluids, *International Journal of Heat and Mass Transfer*, 9–10, 50, (2007), 2002–2018.
- [13] O Makinde. Similarity solution for natural convection from a moving vertical plate with internal heat generation and a convective boundary condition, *Thermal Science*, 15, (2011), 137–143.
- [14] S Mojumder, S Saha and MAH Mamun. Effect of Magnetic Field on Natural Convection in a Cshaped Cavity Filled with Ferrofluid, *Procedia Engineering*, 2014, 105, (2015), 96–104.
- [15] M Sheikholeslami, DD Ganji & MM Rashidi. Ferrofluid flow and heat transfer in a semi annulus enclosure in the presence of magnetic source considering thermal radiation, *Journal of the Taiwan Institute of Chemical Engineers*, 47, (2015), 6–17.
- [16] H Blasius. Grenzschichten in flüssigkeiten mit kleiner reibung, *Zeitschrift für Angewandte Mathematik und Physik*, 56, (1908).